

Pairing by a dynamical interaction in a metal

Andrey V. Chubukov¹ and Artem Abanov²

¹*School of Physics and Astronomy and William I. Fine Theoretical Physics Institute,
University of Minnesota, Minneapolis, MN 55455, USA*

²*Department of Physics, Texas A&M University, College Station, USA*

(Dated: January 7, 2022)

Abstract

We consider pairing of itinerant fermions in a metal near a quantum-critical point (QCP) towards some form of particle-hole order (nematic, spin-density-wave, charge-density-wave, etc). At a QCP, the dominant interaction between fermions comes from exchanging massless fluctuations of a critical order parameter. At low energies, this physics can be described by an effective model with the dynamical electron-electron interaction $V(\Omega_m) \propto 1/|\Omega_m|^\gamma$, up to some upper cutoff Λ . The case $\gamma = 0$ corresponds to BCS theory, and can be solved by summing up geometric series of Cooper logarithms. We show that for a finite γ , the pairing problem is still marginal (i.e., perturbation series are logarithmic), but one needs to go beyond logarithmic approximation to find the pairing instability. We discuss specifics of the pairing at $\gamma > 0$ in some detail and also analyze the marginal case $\gamma = 0+$, when $V(\Omega_m) = \lambda \log(\Lambda/|\Omega_m|)$. We show that in this case the summation of Cooper logarithms does yield the pairing instability at $\lambda \log^2(\Lambda/T_c) = O(1)$, but the logarithmic series are not geometrical. We reformulate the pairing problem in terms of a renormalization group (RG) flow of the coupling, and show that the RG equation is different in the cases $\gamma = 0$, $\gamma = 0+$, and $\gamma > 0$.

I. PREFACE

It is our great pleasure to present this paper for the special issue of JETP devoted to 90th birthday of Igor Ekhievich Dzyaloshinskii. His works on correlated electron systems are of highest scientific quality. He made seminal contributions to quantum magnetism, superconductivity, Fermi-liquid theory, and to other subfields of modern condensed matter physics. In a number of works, including the famous ones on the interplay between d-wave superconductivity and antiferromagnetism at the beginning of “high $-T_c$ era” (Refs. ¹⁻³), Igor Ekhievich used the renormalization group technique to obtain the flow of the couplings upon integrating out fermions with higher energies. In this study, we apply the same RG technique to analyze the pairing instability in systems with critical dynamical pairing interaction. We consider this as a natural extension of his works. Happy birthday, Igor Ekhievich, and the very best wishes.

II. INTRODUCTION.

The pairing near a quantum-critical point (QCP) in a metal and its interplay with non-Fermi-liquid behavior in the normal state, is a fascinating subject, which attracted substantial attention in the correlated electron community after the discovery of superconductivity (SC) in the cuprates, Fe-based systems, heavy-fermion materials, organic materials, and, most recently, twisted bilayer graphene⁴⁻¹⁶. Itinerant QC models, analyzed in recent years, include models of fermions in spatial dimensions $D \leq 3$, various two-dimensional models near zero-momentum spin and charge nematic instabilities, and instabilities towards spin and charge density-wave order with either real or imaginary (current) order parameter, 2D fermions at a half-filled Landau level, Sachdev-Ye-Kitaev (SYK) and SYK-Yukawa models, strong coupling limit of electron-phonon superconductivity, and even color superconductivity of quarks, mediated by gluon exchange. These problems have also been studied analytically and using various numerical techniques. We refer a reader to Ref.¹⁷, where the extensive list of references to these works has been presented.

From theory perspective, pairing near a QCP is a fundamentally novel phenomenon because an effective dynamic electron-electron interaction, $V(q, \Omega)$, mediated by a critical collective boson, which condenses at a QCP, provides a strong attraction in one or more

pairing channels and, at the same time, gives rise to a non-Fermi liquid (NFL) behavior in the normal state. The two tendencies compete with each other: fermionic incoherence, associated with the NFL behavior, destroys the Cooper logarithm and reduces the tendency to pairing, while an opening of a SC gap eliminates the scattering at low energies and reduces the tendency to a NFL. To find the winner of this competition (SC or NFL), one needs to analyze the set of integral equations for the fermionic self-energy, $\bar{\Sigma}(\mathbf{k}, \omega)$, and the gap function, $\Delta(\mathbf{k}, \omega)$, for fermions with momentum/frequency (\mathbf{k}, ω) and $(-\mathbf{k}, -\omega)$.

We consider the subset of models, in which collective bosons are slow modes compared to dressed fermions, for one reason or the other. In this situation, which bears parallels with Eliashberg theory for electron-phonon interaction¹⁸, the self-energy and the pairing vertex can be approximated by their values on the Fermi surface (FS) and computed within the one-loop approximation. The self-energy on the FS, $\bar{\Sigma}(\mathbf{k}_F, \omega)$, is invariant under rotations from the point group of the underlying lattice. The rotational symmetry of the gap function $\Delta(\mathbf{k}_F, \omega)$ and the relation between the phases of $\Delta(\mathbf{k}_F, \omega)$ on different FS's in multi-band systems are model specific. E.g., near an antiferromagnetic QCP in a system with a single FS, the strongest attraction is in the d -wave channel. In each particular case, one has to project the pairing interaction into the irreducible channels, find the strongest one, and solve for the pairing vertex for a given pairing symmetry.

Away from a QCP, the effective $V(\Omega)$ tends to a finite value at $\Omega = 0$. In this situation, the fermionic self-energy has a FL form at the smallest frequencies, and the equation for $\Delta(\omega)$ is similar to that in a conventional Eliashberg theory for phonon-mediated superconductivity; the only qualitative distinction for electronically-mediated pairing is that $V(\Omega)$ by itself changes below T_c due to feedback from fermionic pairing on collective modes. At a QCP, the situation is qualitatively different because the effective interaction $V(\Omega)$, mediated by a critical massless boson, is a singular function of frequency. Quite generally, such interaction behaves at the smallest Ω_m on the Matsubara axis as $V(\Omega_m) \propto 1/|\Omega_m|^\gamma$, where $\gamma > 0$ is some exponent. (Fig. 1). This holds at frequencies below some upper cutoff Λ . At larger $\Omega_m > \Lambda$, the interaction drops even further, and can be safely neglected.

In these notations, BCS pairing corresponds to $\gamma = 0$. The superconducting transition temperature T_c in the BCS case can be most straightforwardly obtained by computing the pairing susceptibility χ_{pp} in the order-by-order expansion in the coupling and identifying the temperature at which it diverges. The series contain the powers of the product of the

Cooper logarithm $\log \Lambda/T_c$ and the dimensionless coupling λ , defined such that $1 + \lambda$ is the ratio of the renormalized and the bare electron masses. The series are geometrical, i.e., $\chi_{pp} = \chi_0(1 + \lambda \log \Lambda/T_c + (\lambda \log \Lambda/T_c)^2 + \dots) = \chi_0/(1 - \lambda \log \Lambda/T_c)$. We will see that for $\gamma > 0$, the pairing kernel still has a marginal $1/|\omega|$ form, and, as a result, the series for χ_{pp} still contain logarithms. However, contrary to the BCS case, where $1/|\omega|$ comes from the fermionic propagator, the marginal exponent -1 for $\gamma > 0$ is the sum of the exponent γ from the interaction and $1 - \gamma$ from the fermionic self-energy (see below). As a result, the logarithmic series are not geometric, and we will see that χ_{pp} does not diverge down to $T = 0$. We show that the pairing instability still exists, however one needs to go beyond the logarithmic approximation to obtain it.

We show that there exists a special case, which falls in between $\gamma = 0$ and $\gamma > 0$. This is the limit $\gamma \rightarrow 0+$, when $V(\Omega_m) \propto \log \Lambda/|\Omega_m|$. In this limit, the pairing instability still can be detected by summing up the series of logarithms for χ_{pp} . However, the series are not geometric, and some extra efforts are needed to sum them up to find the form of χ_{pp} and detect the pairing instability at $T \sim \Lambda e^{-\pi/(2\sqrt{\lambda})}$.

The model with the interaction $V(\Omega_m) \propto 1/|\Omega_m|^\gamma$ displays a very rich physics, and our group has studied it over the last few years. This physics is particularly interesting for $\gamma \leq 2$, where a wide range of the pseudogap (preformed pair) behavior emerges, and for $\gamma > 2$, when the new, non-superconducting ground state emerges¹⁹. In this communication, we will not discuss these values of γ but instead focus on small γ and discuss in some detail the difference between BCS pairing at $\gamma = 0$ and the pairing at $\gamma = 0+$ and at $\gamma > 0$. We derive the Eliashberg equation for the pairing vertex and analyze it within logarithmic perturbation theory and beyond it. We then convert the integral Eliashberg equation into the approximate differential equation and obtain and solve the corresponding renormalization group (RG) equation.

The pairing problem at small γ attracted a lot of attention in the last few years from various physics sub-communities of physicists^{20–34}. The pairing interaction $V(\Omega) \sim 1/|\Omega|^\gamma$ with $\gamma \ll 1$ emerges for fermions near a generic particle-hole instability in a weakly anisotropic 3D system (more explicitly, in dimension $D = 3 - \epsilon$, where $\epsilon \sim \gamma$, Refs. ^{20–22}). A similar gap equation with small γ holds for the pairing in graphene³⁵. The model with $\gamma = 0+$ describes the pairing in 3D systems and color superconductivity of quarks due to gluon exchange^{29,31–33}. The $\gamma = 0+$ model yields a marginal Fermi liquid form of the fermionic

self-energy in the normal state and was argued^{36,37} to be relevant to pairing in the cuprates and, possibly, in Fe-based superconductors.

The structure of the paper is as follows. In the next Section we present the set of coupled Eliashberg equations for the pairing vertex $\Phi(\omega_m)$ and the fermionic self-energy $\bar{\Sigma}(\omega_m)$ and combine them into the equation for the gap function $\Delta(\omega_m)$. In Sec. IV we analyze the structure of the logarithmic perturbation theory for $\gamma = 0+$ and $\gamma > 0$. In Sec. V we go beyond perturbation theory and re-express the integral Eliashberg equation as an approximate differential equation for the pairing vertex and solve it. We show that for $\gamma = 0+$, the solution coincides with the result of summation of logarithmic series. For $\gamma > 0$, we show that the system does become unstable towards pairing if the interaction exceeds a certain threshold. In Sec. VI we analyze the pairing at small γ from RG perspective and reproduce the results of the previous Section. We present our conclusions in Sec. VII.

III. THE MODEL

We consider itinerant fermions at the onset of a long-range particle-hole order in either spin or charge channel. At a critical point, the propagator of a soft boson becomes massless and mediates singular interaction between fermions. A series of earlier works on spin-density-wave order, charge-density-wave order, Ising-nematic order, etc (see Ref.¹⁷ for references) have found that this interaction is attractive in at least one pairing channel. We take this as input and project boson-mediated interaction into the channel with the strongest attraction. As we said, at small frequencies, the interaction scales as $V(\Omega_m) \propto 1/|\Omega_m|^\gamma$. We incorporate dimension-full factors, like the density of states, into $V(\Omega_m)$ and treat it as dimensionless. We assume that the power-law form holds up to the scale Λ , and set $V(\Omega_m) = 0$ above this scale. To keep $V(\Omega_m)$ continuous at Λ and also to transform gradually between $\gamma = 0+$ and $\gamma > 0$, we use the following form for $V(\Omega_m)$ (Fig.1):

$$V(\Omega_m) = \frac{\lambda}{\gamma} \left(\frac{\bar{g}}{|\Omega_m|} \right)^\gamma \left(1 - \left(\frac{|\Omega_m|}{\Lambda} \right)^\gamma \right) \quad (1)$$

Here λ is a dimensionless coupling, and \bar{g} has units of energy. We assume that $\lambda \ll 1$, but the ratio λ/γ can be arbitrary. At $\gamma = 0+$, the last term in (1) can be expanded in γ and yields the logarithmic interaction

$$V(\Omega_m) = \lambda \log \frac{\Lambda}{|\Omega_m|} \quad (2)$$

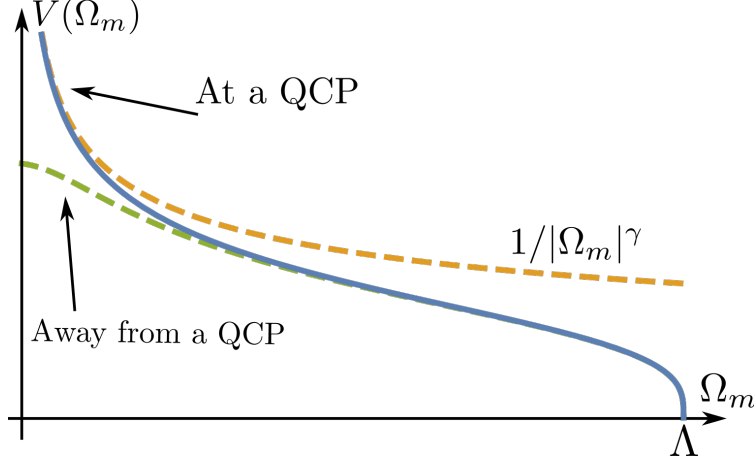


FIG. 1. Frequency dependence of the effective interaction $V(\bar{\Omega}_m)$, mediated by a soft boson, at $T = 0$. Away from a QCP, $V(\bar{\Omega}_m)$ tends to a finite value at $\bar{\Omega}_m = 0$. Right at a QCP, the boson becomes massless, and $V(\bar{\Omega}_m)$ diverges as $1/|\bar{\Omega}_m|^\gamma$.

The conventional BCS/Eliashberg case in this notations is obtained by extending (1) to the case when a pairing boson has a finite mass. In this situation, Ω_m is replaced by a constant below a certain scale. In BCS theory, this scale is assumed to be comparable to Λ , such that $V(\Omega_m) \approx \lambda_{BCS}$ up to $|\Omega_m| \sim \Lambda$, and zero at larger $|\Omega_m|$.

Below we measure all quantities with the dimension of energy, i.e., T, Ω_m, Λ , in units of \bar{g} , i.e., introduce $\bar{T} = T/\bar{g}$, $\bar{\Omega}_m = \Omega_m/\bar{g}$, and $\bar{\Lambda} = \Lambda/\bar{g}$. Throughout this paper we assume that $\bar{\Lambda} \gg 1$.

Earlier works on the pairing mediated by a soft collective boson found that a boson is overdamped due to Landau damping into a particle-hole pair and can be treated as slow mode compared to a fermion, i.e., at the same momentum q , a typical fermionic frequency is much larger than a typical bosonic frequency. This is the same property that justified Eliashberg theory of phonon-mediated superconductivity. By analogy, the theory of electronic superconductivity, mediated by soft collective bosonic excitations in spin or charge channel, is often referred to as Eliashberg theory, and we will be using this convention.

In Eliashberg theory, one can explicitly integrate first over the momentum component perpendicular to the Fermi surface and then over the component(s) along the Fermi surface, and reduce the pairing problem to a set of coupled integral equations for frequency dependent self-energy $\bar{\Sigma}(\omega_m)$ and the pairing vertex $\Phi(\omega_m)$.

At $T = 0$, the coupled Eliashberg equations are

$$\begin{aligned}\bar{\Phi}(\bar{\omega}_m) &= \frac{1}{2} \int d\bar{\omega}'_m \frac{\Phi(\bar{\omega}'_m)}{\sqrt{\tilde{\Sigma}^2(\bar{\omega}'_m) + \bar{\Phi}^2(\bar{\omega}'_m)}} V(|\bar{\omega}_m - \bar{\omega}'_m|), \\ \tilde{\Sigma}(\bar{\omega}_m) &= \bar{\omega}_m + \frac{1}{2} \int d\bar{\omega}'_m \frac{\tilde{\Sigma}(\bar{\omega}'_m)}{\sqrt{\tilde{\Sigma}^2(\bar{\omega}'_m) + \bar{\Phi}^2(\bar{\omega}'_m)}} V(|\bar{\omega}_m - \bar{\omega}'_m|)\end{aligned}\quad (3)$$

where $\tilde{\Sigma}(\bar{\omega}_m) = \bar{\omega}_m + \bar{\Sigma}(\bar{\omega}_m)$. In these equations, both $\bar{\Sigma}(\omega_m)$ and $\bar{\Phi}(\omega_m)$ are real functions. Observe that we define $\bar{\Sigma}(\omega_m)$ with the overall plus sign and without the overall factor of i . In the normal state ($\bar{\Phi} \equiv 0$), we have at $\gamma > 0$, and $|\bar{\omega}_m| \ll 1$

$$\tilde{\Sigma}(\bar{\omega}_m) = \bar{\omega}_m + \frac{|\bar{\omega}_m|^{1-\gamma}}{1-\gamma} \text{sgn } \bar{\omega}_m, \quad (4)$$

At $\gamma = 0+$,

$$\tilde{\Sigma}(\omega_m) = \bar{\omega}_m \left(1 + \lambda \log \frac{\bar{\Lambda}}{|\bar{\omega}_m|} \right), \quad (5)$$

The superconducting gap function $\bar{\Delta}(\bar{\omega}_m)$ is defined as the ratio

$$\bar{\Delta}(\bar{\omega}_m) = \bar{\omega}_m \frac{\bar{\Phi}(\bar{\omega}_m)}{\tilde{\Sigma}(\bar{\omega}_m)} = \frac{\bar{\Phi}(\bar{\omega}_m)}{1 + \bar{\Sigma}(\bar{\omega}_m)/\bar{\omega}_m}. \quad (6)$$

The equation for $\bar{\Delta}(\omega_m)$ is readily obtained from (3):

$$\bar{\Delta}(\bar{\omega}_m) = \frac{1}{2} \int d\bar{\omega}'_m \frac{\bar{\Delta}(\bar{\omega}'_m) - \bar{\Delta}(\bar{\omega}_m) \frac{\bar{\omega}'_m}{\bar{\omega}_m}}{\sqrt{(\bar{\omega}'_m)^2 + \bar{\Delta}^2(\bar{\omega}'_m)}} \frac{1}{|\bar{\omega}_m - \bar{\omega}'_m|^\gamma}. \quad (7)$$

This equation contains a single function $\bar{\Delta}(\bar{\omega}_m)$, but for the cost that $\bar{\Delta}(\bar{\omega}_m)$ appears also in the r.h.s., which makes Eq. (7) less convenient for the analysis than Eqs. (3).

For a generic $\gamma > 0$, the coupled equations (3) for $\bar{\Phi}$ and $\tilde{\Sigma}$ describe the interplay between the two competing tendencies – one towards superconductivity, specified by $\bar{\Phi}$, and the other towards incoherent NFL normal-state behavior, specified by $\tilde{\Sigma}$. The competition between the two tendencies is encoded in the fact that $\tilde{\Sigma}$ appears in the denominator of the equation for $\bar{\Phi}$ and $\bar{\Phi}$ appears in the denominator of the equation for $\tilde{\Sigma}$. In more physical terms, a self-energy $\tilde{\Sigma}$ is an obstacle to Cooper pairing, while when $\bar{\Phi}$ is non-zero, it reduces the strength of the self-energy and renders fermionic coherence.

The full set of the equations for electron-mediated pairing generally must contain the third equation, describing the feedback from the pairing on the bosonic propagator. This feedback is small in the case of electron-phonon interaction, but is generally not small when

the pairing is mediated by a collective mode because the dispersion of a collective mode changes qualitatively below T_c (Refs.^{38,39}). In this work, we only consider the computation of T_c and will not discuss system behavior below T_c . For this computation, it is sufficient to restrict with the two equations (3). Moreover, we can (i) treat $\bar{\Phi}(\bar{\omega}_m)$ as infinitesimally small and neglect it in the denominator of Eq. (3), and (ii) use Eqs. (4) or (5) for $\bar{\Sigma}$. For a small, but finite $\gamma > 0$, the linearized equation for the pairing vertex is

$$\bar{\Phi}(\bar{\omega}_m) = \frac{1}{2} \int d\bar{\omega}'_m \frac{\bar{\Phi}(\bar{\omega}'_m)}{|\bar{\omega}'_m|^{1-\gamma} |\bar{\omega}_m - \bar{\omega}'_m|^\gamma (1 + (\gamma/\lambda) |\bar{\omega}'_m|^\gamma)} \left(1 - \left(\frac{|\bar{\omega}_m - \bar{\omega}'_m|}{\bar{\Lambda}} \right)^\gamma \right) \quad (8)$$

Observe that the overall coupling is just a number, equal to one, because the factor λ/γ in $V(\bar{\Omega}_m)$ cancels out with the same factor in the self-energy. This factor is still present in the denominator, but in the term, which contains $|\bar{\omega}'_m|^\gamma$ and becomes irrelevant at the smallest frequencies

At $\gamma = 0+$, the linearized equation for $\bar{\Phi}(\bar{\omega}_m)$ is

$$\bar{\Phi}(\bar{\omega}_m) = \frac{\lambda}{2} \int d\bar{\omega}'_m \frac{\bar{\Phi}(\bar{\omega}'_m)}{|\bar{\omega}'_m|} \frac{\log \frac{\bar{\Lambda}}{|\bar{\omega}_m - \bar{\omega}'_m|}}{1 + \lambda \log \frac{\bar{\Lambda}}{|\bar{\omega}_m - \bar{\omega}'_m|}} \quad (9)$$

IV. SUMMING UP THE LOGARITHMS

As a first try, we analyze the linearized equation for the pairing vertex perturbatively, by adding up a trial, infinitesimally small $\bar{\Phi}_0$ to the r.h.s of Eqs. (8) and (9) and computing the pairing susceptibility perturbatively, order-by-order. Such approach has been commonly used for BCS pairing. The perturbation series there contain singular Cooper logarithms. The logarithmic singularity can be cut either by a finite T or at $T = 0$, by a finite total incoming bosonic frequency, $\bar{\Omega}_{tot}$. For consistency with other cases, we set $T = 0$ and keep $\bar{\Omega}_{tot}$ finite. The result of order-by-order analysis for a BCS pairing is well known:

$$\bar{\Phi}(\bar{\Omega}_{tot}) = \bar{\Phi}_0 \left(1 + \lambda_{BCS} \log \frac{\bar{\Lambda}}{|\bar{\Omega}_{tot}|} + \lambda_{BCS}^2 \log^2 \frac{\bar{\Lambda}}{|\bar{\Omega}_{tot}|} + \dots \right) = \frac{\bar{\Phi}_0}{1 - \lambda_{BCS} \log \frac{\bar{\Lambda}}{|\bar{\Omega}_{tot}|}} \quad (10)$$

The ratio $\bar{\Phi}(\bar{\Omega}_{tot})/\bar{\Phi}_0$ (the pairing susceptibility) diverges at $|\bar{\Omega}_{tot}| = \bar{\Lambda}e^{-1/\lambda_{BCS}}$ and becomes negative at smaller $|\bar{\Omega}_{tot}|$, indicating that the normal state is unstable towards pairing. (In a more accurate description, the pole in $\bar{\Phi}(\bar{\Omega}_{tot})$ moves from the lower to the upper half-plane of complex frequency⁴⁰).

We now do the same calculation for $\gamma > 0$. The kernel in Eq. (8) is still marginal at $\bar{\omega}'_m, \bar{\omega}_m \ll 1$, but, as we said, now the scaling dimension -1 is the sum of $-\gamma$, coming from the

interaction, and $-1 + \gamma$, coming from the self-energy. This implies that perturbation theory still contains logarithms, but in distinction to BCS, each logarithmical integral $\int d\bar{\omega}'_m/|\bar{\omega}'_m|$ runs between the upper cutoff at $|\bar{\omega}'_m| \sim \bar{\omega}_{max} = (\lambda/\gamma)^{1/\gamma}$ and the lower cutoff at $|\bar{\omega}'_m| \sim |\bar{\omega}_m|$. Because the lower cutoff is finite, we can set $\bar{\Omega}_{tot} = 0$. Summing up the logarithmical series, we then obtain⁴¹

$$\bar{\Phi}(\bar{\omega}_m) = \bar{\Phi}_0 \left(1 + \log \frac{\bar{\omega}_{max}}{|\bar{\omega}_m|} + \frac{1}{2} \log^2 \frac{\bar{\omega}_{max}}{|\bar{\omega}_m|} + \dots \right) = \bar{\Phi}_0 e^{\log \bar{\omega}_{max}/|\bar{\omega}_m|} = \bar{\Phi}_0 \frac{\bar{\omega}_{max}}{|\bar{\omega}_m|} \quad (11)$$

We see that the pairing susceptibility increases as $\bar{\omega}_m$ decreases, but remains finite and positive for all finite $\bar{\omega}_m$, even when $\bar{\Omega}_{tot} = 0$. Re-doing calculations at a finite $\bar{\Omega}_{tot}$ we find the same result as in (11), with $|\bar{\omega}_m|$ replaced by $\max(|\bar{\omega}_m|, \bar{\Omega}_{tot})$. This implies that for $\gamma > 0$, there is no signature of a pairing instability within the logarithmic approximation. The absence of a pairing instability within the logarithmic approximation generally implies that pairing does not develop at weak coupling and, if exists, is a threshold phenomenon. In our case, the dimensionless coupling in the series in Eq. (11) is a number equal to one, i.e., the problem we consider is not weak-coupling. A weak-coupling limit can be reached if we extend the model and make the pairing interaction parametrically smaller than the one in the particle-hole channel. In practice, this is done by multiplying the interaction in the pairing channel by $1/N$, where $N > 1$ (Refs.^{17,22,34,42,43}), while the interaction in the particle-hole channel is left intact⁴⁴ In the extended model, $\log \bar{\omega}_{max}/|\bar{\omega}_m|$ gets multiplied by $1/N$, and at large N the problem becomes weak-coupling. We show below that indeed there is no pairing instability at large N .

The case $\gamma = 0+$ falls in between BCS and $\gamma > 0$ cases. Namely, we show below that the series of logarithms are not geometric, like the ones for $\gamma > 0$, however by summing up the series one does find the scale of a pairing instability, like in BCS. We assume and then verify that for relevant $\bar{\omega}'_m$, $\lambda \log(\bar{\Lambda}/|\bar{\omega}'_m|)$ is small for $\lambda \ll 1$, and neglect this term in the denominator of (9). We keep $\bar{\Omega}_{tot}$ non-zero to avoid divergencies and for simplicity set $\bar{\omega}_m$ and $\bar{\Omega}_{tot}$ to be comparable. To logarithmic accuracy, we can then view $\bar{\Phi}$ as a function of a single parameter $\bar{\Omega}_{tot}$.

Because the interaction is logarithmic, perturbation series hold in $\lambda \log^2(\bar{\Lambda}/|\bar{\omega}_m|)$. Evaluating the pairing vertex in order-by-order calculations, we find (see Appendix for details)

$$\bar{\Phi}(\bar{\Omega}_{tot}) = \bar{\Phi}_0 \left(1 + \frac{1}{2} \lambda \log^2 \frac{\bar{\Lambda}}{|\bar{\Omega}_{tot}|} + \frac{5}{24} \lambda^2 \log^4 \frac{\bar{\Lambda}}{|\bar{\Omega}_{tot}|} + \frac{61}{720} \lambda^3 \log^6 \frac{\bar{\Lambda}}{|\bar{\Omega}_{tot}|} + \dots \right) \quad (12)$$

At a first glance, the coefficients in (12) are just some uncorrelated numbers. On a more careful look, we realize that the series fall into

$$\bar{\Phi}(\bar{\Omega}_{tot}) = \bar{\Phi}_0 \frac{1}{\cos\left(\sqrt{\lambda} \log(\bar{\Lambda}/|\bar{\Omega}_{tot}|)\right)} \quad (13)$$

Accordingly, the pairing susceptibility diverges when the argument of \cos becomes $\pi/2$, i.e., at $\bar{\Omega}_{tot} = \bar{\Lambda}e^{-\pi/2\sqrt{\lambda}}$. It is natural to associate this scale with T_c (Ref.²⁹). The susceptibility also diverges at a set of smaller $\bar{\Omega}_{tot,n} = \bar{\Lambda}e^{-\pi(1+2n)/2\sqrt{\lambda}}$, but here we focus only on the highest onset temperature. We see that T_c has exponential dependence on the coupling, like in BCS theory, however the argument of the exponent contains $\sqrt{\lambda}$ rather than λ . This in turn justifies the neglect of the self-energy, because for relevant frequencies, $\lambda \log(\bar{\Lambda}/|\bar{\omega}'_m|) \sim \sqrt{\lambda} \ll 1$ (the corrections due to self-energy have been analyzed in Ref.³³).

To summarize, the case $\gamma = 0+$ is similar to BCS in the sense that pairing occurs for arbitrary weak coupling (T_c remains finite even if we replace λ by λ/N and set N to be large). However, for and finite $\gamma > 0$, there is no indication of the pairing instability within the logarithmic approximation.

V. THE DIFFERENTIAL EQUATION FOR $\bar{\Phi}(\bar{\omega}_m)$

We now analyze the linearized equation for the pairing vertex for $\gamma > 0$ beyond the logarithmic approximation. To do this, we convert integral equation (8) into to a differential equation with certain boundary conditions and solve it non-perturbatively.

A. The case $\bar{\Lambda} = \infty$

We first consider the case $\Lambda = \infty$. We keep $N \geq 1$ as a parameter, as we need to verify our earlier conjecture that there is no pairing instability for large enough N . To convert (8) into differential equation, we use the fact that at small γ , the integral in the r.h.s. of (8) predominantly comes from internal $\bar{\omega}'_m$, which are either substantially larger or substantially smaller than the external $\bar{\omega}_m$. We then split the integral over $\bar{\omega}'_m$ into two parts: in one we approximate $|\bar{\omega}_m - \bar{\omega}'_m|$ by $|\bar{\omega}'_m|$, in the other by $|\bar{\omega}_m|$. Introducing $z = |\bar{\omega}_m|^\gamma$, we then simplify (8) to

$$\bar{\Phi}(z) = \frac{1}{N\gamma} \left[\int_z^\infty dy \frac{\bar{\Phi}(y)}{y(1+\alpha y)} + \frac{1}{z} \int_0^z dy \frac{\bar{\Phi}(y)}{1+\alpha y} \right] \quad (14)$$

where $\alpha = \gamma/\lambda$ ($\bar{\omega}_{max} = (1/\alpha)^{1/\gamma}$). Differentiating this equation twice over z and replacing $\bar{\Phi}(z)$ by $\bar{\Delta}(z) = \alpha\bar{\Phi}(z)z/(1+\alpha z)$, we obtain the second order differential gap equation in the form (Refs. ^{17,24,25,42})

$$(\bar{\Delta}_{\text{diff}}(z)(1+\alpha z))'' = - (1/4 - b_N^2) \frac{\bar{\Delta}_{\text{diff}}(z)}{z^2}, \quad (15)$$

where $(\dots)'' = d^2(\dots)/dz^2$ and

$$b_N = \sqrt{\frac{1}{4} - \frac{1}{\gamma N}} \quad (16)$$

This $\bar{\Delta}_{\text{diff}}(z)$ has to be real and satisfy the boundary conditions at large z and at $z = 0$. At large z , we expect perturbation theory to work, hence $\lim_{z \rightarrow \infty} \bar{\Delta}_{\text{diff}}(z) = \bar{\Phi}_0$. The boundary condition at $z = 0$ is set by the requirement that $\bar{\Delta}_{\text{diff}}(z)$ is normalizable, i.e., that the ground state energy for a non-zero $\bar{\Delta}_{\text{diff}}(z)$ must be free from divergencies. This requirement imposes the condition that $\int dz (\bar{\Delta}_{\text{diff}}^2(z)/z^2)$ should be infra-red convergent (Refs.^{17,45}).

The solution of (15) is expressed via a Hypergeometric function, and the form of $\bar{\Delta}_{\text{diff}}(z)$ depends on whether b_N is real or imaginary, i.e., whether N is larger or smaller than $N_{cr} = 4/\gamma$. When $N > N_{cr}$, b_N is real, and the solution is

$$\bar{\Delta}_{\text{diff}}(z) = C_1 S[b_N, z] + C_2 S[-b_N, z] \quad (17)$$

where

$$S[b_N, z] = z^{b_N+1/2} {}_2F_1 \left[\frac{1}{2} + b_N, \frac{3}{2} + b_N, 1 + 2b_N, -\alpha z \right]. \quad (18)$$

Both $S[b_N, z]$ and $S[-b_N, z]$ are sign-preserving functions. At small z , $S[\pm b_N, z] \approx z^{1/2 \pm b_N}$, and at large z , $S[\pm b_N, z]$ tend to finite values $\frac{4^{\pm b_N} \Gamma(1 \pm b_N)}{\sqrt{\pi} \Gamma(\frac{3}{2} \pm b_N)}$. The boundary condition at $z = 0$ sets $C_2 = 0$, and the one at $z \gg 1$ sets the linear relation between C_1 and $\bar{\Phi}_0$. We plot $\bar{\Delta}_{\text{diff}}(z)$ for $b_N = 0.2$ and $\alpha = 1$ in Fig. 2. We see that $\bar{\Delta}_{\text{diff}}(z)$ remains positive for all z , i.e., the normal state remains stable with respect to pairing. At $\gamma N \gg 1$, $b_N \approx 1/2 - 1/(\gamma N)$, and $\bar{\Delta}_{\text{diff}}(z)/\bar{\Phi}_0 \propto 1/|z|^{1/(N\gamma)}$. This is the same result that we obtained by summing up the logarithms. We see that in this parameter range the non-logarithmic terms just change the exponent from $1/N$ to $(\gamma/2)\sqrt{1 - 4/(N\gamma)}$.

This behavior holds as long as b_N is real, i.e., $N > N_{cr} = 4/\gamma$. For models with smaller $N < N_{cr}$, including our original model with $N = 1$, b_N is imaginary, $b_N = i\beta_N$, where $\beta_N = \sqrt{1/(N\gamma) - 1/4} = (1/N\gamma)^{1/2}(1 - N/N_{cr})^{1/2}$. In this situation, the solution of the differential equation is

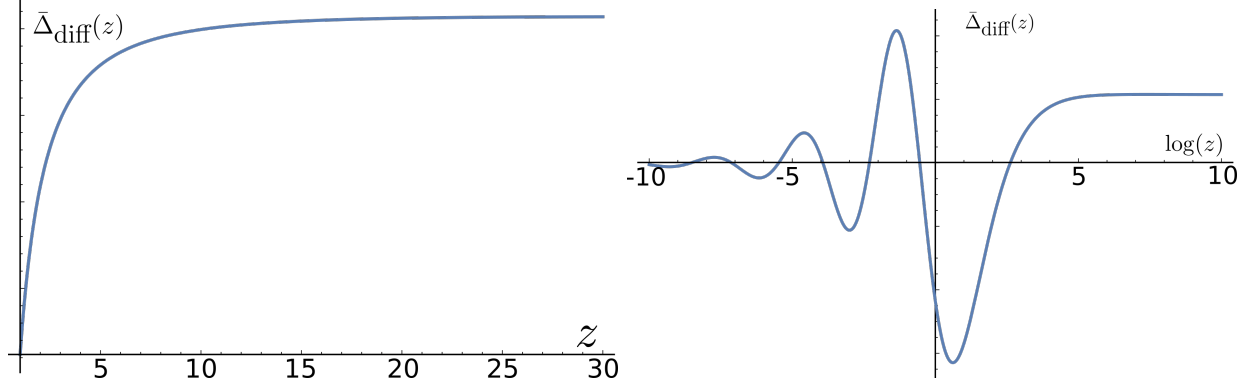


FIG. 2. Left: The function $\bar{\Delta}_{\text{diff}}(z)$, Eq. (17), for real $b_N = 0.2$ ($N > N_{cr}$) and $\alpha = 1$. Right: the same function for imaginary $b_N = 2i$ ($N < N_{cr}$). For real b_N perturbation theory around the normal state is regular, which indicates that there is no pairing instability. For imaginary $b_N = i\beta_N$, $\bar{\Delta}_{\text{diff}}(z)$ oscillates at small z . We argue in the text that this implies that the normal state becomes unstable towards pairing.

$$\bar{\Delta}_{\text{diff}}(z) = C\sqrt{z} \times \text{Re} \left(e^{i\psi} z^{i\beta_N} {}_2F_1 \left[\frac{1}{2} + i\beta_N, \frac{3}{2} + i\beta_N, 1 + 2i\beta_N, -\alpha z \right] \right) \quad (19)$$

The boundary condition at $z = 0$ is satisfied as at small z , $\bar{\Phi}_{\text{diff}}(z)$ acquires a form of a free quantum particle with a "coordinate" $x = \log z$. At $z \gg 1$, $\bar{\Delta}_{\text{diff}}(z)$ tends to a constant for a generic ψ , and the boundary condition sets up a linear relation between C and $\bar{\Phi}_0$.

We plot $\bar{\Delta}_{\text{diff}}(z)$ in Fig. (2). We see that the gap function now passes through a minimum at some z^* and oscillates at smaller z . The oscillating behavior at $z < z^*$ could not be obtained within perturbation theory starting from $\bar{\Phi}(z) = \bar{\Phi}_0$ as the kernel in Eq. (8) is entirely positive. This strongly suggests that the normal state is now unstable towards pairing, and $(z^*)^{1/\gamma}$ sets the value of \bar{T}_c . To verify this, in Ref. ⁴⁶ we solved the gap equation at a finite T . This calculation is a bit more tricky due to special behavior of fermions with Matsubara frequencies $\omega_m = \pm\pi T$, but nevertheless it confirms the two key points of our $T = 0$ analysis that superconducting \bar{T}_c is finite and is generally of order z^* .

Note that the value of z^* depends on the magnitude of β_N , i.e., on the ratio N_{cr}/N . For small β_N , which holds when N is only slightly below N_{cr} , the first sign change of $\chi_{pp}(z) \equiv \bar{\Delta}_{\text{diff}}/\bar{\Phi}_0$ occurs at small $z^* \sim e^{-a/\beta_N}$, where $a = O(1)$. For larger β_N , the first sign change occurs at $\alpha z^* \sim 1/(N\gamma) \geq 1$, i.e., at $z^* \sim \lambda/N\gamma^2$, or, equivalently, at $\bar{\omega}_m \sim \bar{\omega}_{max}(1/(N\gamma))^{1/\gamma}$.

This holds for the original model with $N = 1$.

We note in passing that $\bar{\Delta}_{\text{diff}}(z)$ contains two parameters: the overall factor C and the phase factor ψ . The boundary condition at $z \gg 1$ then still leaves the freedom of, e.g., choosing ψ for a given $C \sim \bar{\Phi}_0$. This extra freedom comes about because it turns out¹⁷ that the homogeneous gap equation (the one without $\bar{\Phi}_0 = 0$) by itself has a non-zero solution at $T = 0$, such that $\bar{\Delta}_{\text{diff}}(z)$ is the sum of the induced and the homogeneous solutions of (8). To demonstrate this more explicitly, we set $z > 1/\alpha$, use the fact that in this range a hypergeometric function reduces to a combination of Bessel and Neumann functions, and re-express (19) as

$$\bar{\Delta}_{\text{diff}}(z) \sim \frac{1}{\sqrt{z}} \left[A_1 J_1 \left(\sqrt{\frac{4\beta_N^2 + 1}{\alpha z}} \right) + A_2 Y_1 \left(\sqrt{\frac{4\beta_N^2 + 1}{\alpha z}} \right) \right], \quad (20)$$

where J_1 and Y_1 are Bessel and Neumann functions, respectively. At small value of the argument, $J_1(p) \approx p$ and $Y_1(p) \approx 1/p$, i.e., the first term vanishes at large z , while the second one tends to a constant. Then A_2 is uniquely determined by the boundary condition set by $\bar{\Phi}_0$, while the A_1 piece is the solution of the equation without $\bar{\Phi}_0$.

The existence of the solution of the linearized gap equation at $T = 0$ (well below T_c) is a highly non-trivial feature of pairing at a QCP, that affects fluctuation corrections to superconducting order parameter. For our purposes, however, we only need to analyze only the induced solution to get an estimate of T_c . We can set $A_1 = 0$ in (20) and determine A_2 from the boundary condition at $z \rightarrow \infty$.

B. The case of a finite $\bar{\Lambda}$

At this stage, we have two different energy scales, which we identified with T_c . Namely, at a finite $\bar{\Lambda}$ and $\gamma \rightarrow 0$, we found $\bar{T}_c \sim \bar{\Lambda} e^{-\pi/(2\sqrt{\lambda})}$. At $\bar{\Lambda} \rightarrow \infty$ and finite γ , we found $\bar{T}_c \sim \bar{\omega}_{\text{max}}(1/N\gamma)^{1/\gamma}$. We now analyze the crossover between the two energies. For definiteness, we consider the original model with $N = 1$.

We argued earlier that for the pairing at $\gamma = 0+$, fermions can be treated as free quasi-particles, because for relevant fermions the ratio $\bar{\Sigma}(\bar{\omega}_m)/\bar{\omega}_m \sim \sqrt{\lambda} \ll 1$. The same holds for the case $\bar{\Lambda} = \infty$ and $\gamma > 0$. Here, the ratio $\bar{\Sigma}(\bar{\omega}_m)/\bar{\omega}_m \sim 1/(\alpha z)$, and for $z \sim z^*$, $\bar{\Sigma}(\bar{\omega}_m)/\bar{\omega}_m \sim \gamma \ll 1$. We now use this simplification and re-analyze the differential equation for $\bar{\Delta}(z)$ at a finite $\bar{\Lambda}$.

One can verify that the differential equation retains the same form as for $\bar{\Lambda} = \infty$:

$$(\bar{\Delta}_{\text{diff}}(z)z)'' = -\frac{\lambda}{\gamma^2} \frac{\bar{\Delta}_{\text{diff}}(z)}{z^2}, \quad (21)$$

and its solution is still a linear combination of Bessel and Neumann functions, Eq. (20).

However, we have an extra requirement

$$\bar{\Delta}_{\text{diff}}(\bar{\Lambda}^*) = 0, \quad (22)$$

where $\bar{\Lambda}^* = (\bar{\Lambda})^\gamma$. There is no solution of the homogeneous equation at a finite $\bar{\Lambda}$, and Eq. (22) together with the boundary condition $\bar{\Delta}_{\text{diff}}(\infty) = \bar{\Phi}_0$ uniquely specify the coefficients A_1 and A_2 in (20):

$$\bar{\Delta}_{\text{diff}}(z) = \frac{C}{\sqrt{z}} \times \left[J_1 \left(\frac{2}{(\gamma\alpha z)^{1/2}} \right) Y_1 \left(\frac{2}{(\gamma\alpha\bar{\Lambda}^*)^{1/2}} \right) - Y_1 \left(\frac{2}{(\gamma\alpha z)^{1/2}} \right) J_1 \left(\frac{2}{(\gamma\alpha\bar{\Lambda}^*)^{1/2}} \right) \right], \quad (23)$$

where $C \sim \bar{\Phi}_0$. It is convenient to introduce a dimensionless parameter

$$B = \gamma\alpha\bar{\Lambda}^* = \frac{\gamma^2}{\lambda} (\bar{\Lambda})^\gamma. \quad (24)$$

In the left panel of Fig. 3 we plot $\bar{\Delta}_{\text{diff}}(\bar{\omega}_m)$ for a representative $B = 0.3$. We see that the gap function is regular at $|\bar{\omega}_m| \leq \bar{\Lambda}$, but passes through an extremum and oscillates at smaller $\bar{\omega}_m$. The position of the first extremum depends on B . We now show that the two forms of \bar{T}_c , which we found earlier, correspond to the limits $B \ll 1$ and $B \gg 1$.

When $B \ll 1$, one can use the forms of Bessel and Neumann functions at large argument,

$$\begin{aligned} J_1(x) &\approx \sqrt{\frac{2}{\pi x}} \cos(x - 3\pi/4), \\ Y_1(x) &\approx \sqrt{\frac{2}{\pi x}} \sin(x - 3\pi/4), \end{aligned} \quad (25)$$

and obtain

$$\bar{\Delta}_{\text{diff}}(z) \propto \frac{\bar{\Phi}_0}{z^{1/4}} \sin \left(\frac{2}{B^{1/2}} - \frac{2}{(\alpha\gamma z)^{1/2}} \right) = \frac{C}{z^{1/4}} \sin \frac{2}{B^{1/2}} \left(1 - \left(\frac{\bar{\Lambda}^*}{z} \right)^{1/2} \right) \quad (26)$$

In the original variables $\bar{\omega}_m$ and Λ , this reduces, to the leading order in γ , to

$$\bar{\Delta}_{\text{diff}}(\bar{\omega}_m) \propto \frac{\bar{\Phi}_0}{|\bar{\omega}_m|^{\gamma/4}} \sin \left(\sqrt{\lambda} \log \frac{|\bar{\omega}_m|}{\Lambda} \right). \quad (27)$$

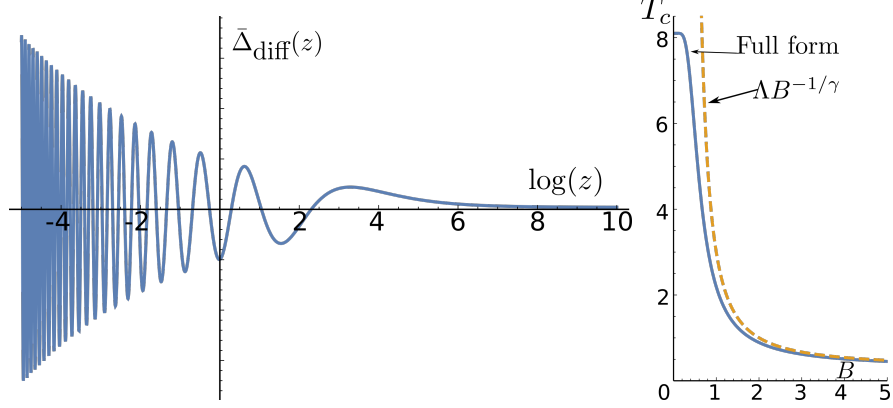


FIG. 3. Left: $\bar{\Delta}_{\text{diff}}(z)$ from (23) for $B = 0.3$, and $\bar{\Lambda}^* = 10$. Right: the sketch of the evolution of T_c as a function of B .

Associating \bar{T}_c with the position of the first extremum of $\bar{\Delta}_{\text{diff}}(\bar{\omega}_m)$, we find $\bar{T}_c \sim \bar{\Lambda} e^{-\pi/(2\sqrt{\bar{\Lambda}})}$. This coincides with the estimate of \bar{T}_c from the analysis of the pairing susceptibility as a function of the total frequency of two fermions in a pair (see Eq. (13)).

In the opposite limit $B \gg 1$, we use $J_1(2/B^{1/2}) \sim 1/B^{1/2}$ and $Y_1(2/B^{1/2}) \sim B^{1/2}$ and keep only $Y_1(2/B^{1/2})$. We then obtain from (23) that the dependence on $\bar{\Lambda}$ appears only in the overall factor:

$$\bar{\Delta}_{\text{diff}}(z) \propto \frac{1}{\sqrt{z}} J_1 \left(\frac{2}{(\gamma \alpha z)^{1/2}} \right), \quad (28)$$

or, in terms of $\bar{\omega}_m$,

$$\bar{\Delta}_{\text{diff}}(\bar{\omega}_m) \propto \frac{1}{|\bar{\omega}_m|^{\gamma/2}} J_1 \left(\frac{2}{B^{1/2}} \left(\frac{\bar{\Lambda}}{|\bar{\omega}_m|} \right)^{\gamma/2} \right) \quad (29)$$

The first extremum is now located at $\bar{\omega}_m^* = (z^*)^{1/\gamma} \sim \bar{T}_c \sim \bar{\Lambda}/B^{1/\gamma}$, i.e., $\bar{T}_c \sim (\lambda/\gamma)^{1/\gamma} (1/\gamma)^{1/\gamma}$. This agrees with the analysis at $\bar{\Lambda} = \infty$.

In the right panel in Fig. 3 we sketch the evolution of \bar{T}_c as a function of B . In terms of B , \bar{T}_c scales as $\bar{\Lambda}/B^{1/\gamma}$ for $B \gg 1$ (the limit of large $\bar{\Lambda}$ and finite γ), and saturates at $\Lambda e^{-\pi/(2\sqrt{\bar{\Lambda}})}$ for $B \ll 1$ (the limit $\gamma = 0+$ and finite $\bar{\Lambda}$). The crossover between the two regimes occurs at $B \sim e^{\pi\gamma/(2\sqrt{\bar{\Lambda}})} \approx 1$.

We note in passing that Eq. (27) could also be obtained directly, by converting the gap equation for $\gamma = 0+$ into the differential equation³⁰. For this we depart from Eq. (9), neglect the self-energy term in the denominator, split the integral over ω'_m into contributions from $\omega'_m \gg \omega_m$ and $\omega'_m \ll \omega_m$, as we did in the derivation of (14), and introduce logarithmic

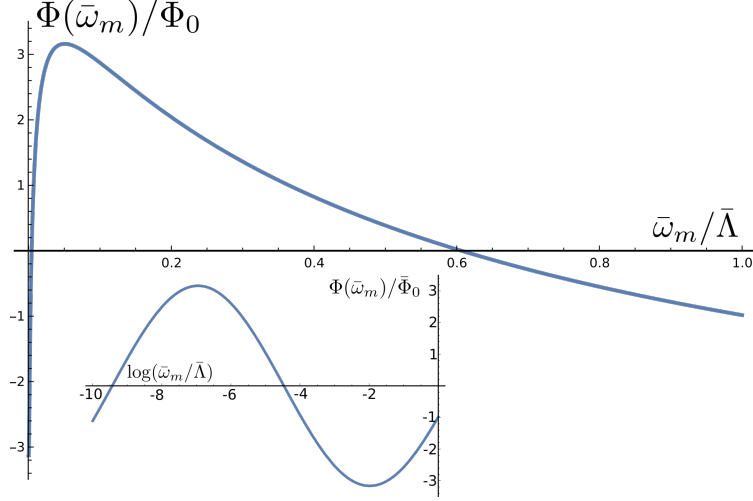


FIG. 4. The function $\Phi(\bar{\omega}_m)$ from Eq. (33). It passes through a maximum at $\bar{\omega}_m \sim \bar{T}_c \sim \bar{\Lambda}e^{-\pi/(2\sqrt{\lambda})}$ and oscillates at smaller $\bar{\omega}_m$ as a simple trigonometric function of $\log \frac{\bar{\Lambda}}{|\bar{\omega}_m|}$ (shown in the insert).

variables $x = \log \Lambda/|\omega_m| = \log \bar{\Lambda}/|\bar{\omega}_m|$, $x' = \log \bar{\Lambda}/|\bar{\omega}'_m|$. We then obtain

$$\Phi(x) = \lambda \left[\int_0^x dx' x' \Phi(x') + x \int_x^\infty dx' \Phi(x') \right] \quad (30)$$

Differentiating twice over x and introducing $y = \gamma x$, we obtain

$$\Phi''(y) = -\frac{\lambda}{\gamma^2} \Phi(y) \quad (31)$$

This equation is valid only for $0 < y < \gamma^2/\lambda$, and the two boundary conditions are $\Phi(y = 0) = \Phi_0$ and $\Phi(y = \gamma^2/\lambda) = 0$. The solution of (31), which satisfies the boundary conditions, is, for small λ ,

$$\Phi(y) = -\bar{\Phi}_0 \frac{\sqrt{\lambda}}{\gamma} \sin \left(\frac{\sqrt{\lambda}}{\gamma} \left(y - \frac{\gamma^2}{\lambda} \right) \right) \quad (32)$$

In the original units, this becomes

$$\Phi(\bar{\omega}_m) = -\bar{\Phi}_0 \frac{\sqrt{\lambda}}{\gamma} \sin \left(\sqrt{\lambda} \log \frac{\bar{\Lambda}}{|\bar{\omega}_m|} - \frac{\gamma}{\sqrt{\lambda}} \right) \quad (33)$$

We plot $\Phi(\bar{\omega}_m)$ in Fig. 4. We see that $\Phi(\bar{\omega}_m)$ is sign-preserving when $\log \frac{\bar{\Lambda}}{|\bar{\omega}_m|}$ is small, but oscillates when $\log \frac{\bar{\Lambda}}{|\bar{\omega}_m|}$ gets larger. Associating the position of the first extremum of $\Phi(\bar{\omega}_m)$ with \bar{T}_c , as we did before, we find the same $\bar{T}_c \sim \bar{\Lambda}e^{-\pi/(2\sqrt{\lambda})}$ as at $B \ll 1$ in our earlier treatment.

VI. RG ANALYSIS

The difference between $\gamma = 0+$ and at a finite γ can be also understood by analyzing the flow of the running 4-fermion pairing vertex within the RG formalism. The RG equations for small $\gamma > 0$ have been derived in Refs. ^{21,24} and for $\gamma = 0+$ in Ref. ²⁹ (see also Refs. ^{31,32}).

The key point for the RG analysis is that at small but finite γ , the interaction $V(\bar{\Omega}_m)$ in (1) can be approximated by

$$V(\bar{\Omega}_m) = \frac{\lambda}{|\bar{\Omega}_m|^\gamma} \log \frac{\bar{\Lambda}}{|\bar{\Omega}_m|} \quad (34)$$

and both the logarithmic and the power-law dependence have to be kept. This interaction can be further re-expressed in terms of $L = \log \frac{\bar{\Lambda}}{|\bar{\Omega}_m|}$ as the product of L and the running effective $\tilde{V}(L) = \tilde{V}(0)e^{\gamma L}$, where $\tilde{V}(0) = \lambda(1/\bar{\Lambda})^\gamma = \gamma^2/B$.

The interaction $V(L) = \tilde{V}(L)L$ acts as the source for the running 4-fermion pairing vertex, which we label as $V_{SC}(L)$. Without the source, $V_{SC}(L)$ would obey a BCS RG equation $\dot{V}_{SC}(L) = V_{SC}^2(L)$. With the source, the equation becomes

$$\dot{V}_{SC}(L) = V_{SC}^2(L) + \tilde{V}(L) \quad (35)$$

The solution of this equation, subject to $V_{SC}(0) = 0$ (no pairing without the source), is ^{21,24}

$$V_{SC}(L) = \frac{\gamma}{B^{1/2}} e^{\gamma L/2} \frac{J_1\left(\frac{2}{B^{1/2}} e^{\gamma L/2}\right) Y_1\left(\frac{2}{B^{1/2}}\right) - Y_1\left(\frac{2}{B^{1/2}} e^{\gamma L/2}\right) J_1\left(\frac{2}{B^{1/2}}\right)}{J_0\left(\frac{2}{B^{1/2}} e^{\gamma L/2}\right) Y_1\left(\frac{2}{B^{1/2}}\right) - Y_0\left(\frac{2}{B^{1/2}} e^{\gamma L/2}\right) J_1\left(\frac{2}{B^{1/2}}\right)} \quad (36)$$

For $B \ll 1$, relevant values of the arguments of Bessel and Neumann functions are large, and using their asymptotic forms, Eq. (25), we find that, to leading order in γ ,

$$V_{SC}(L) \propto \tan(\sqrt{\lambda}L) \quad (37)$$

The 4-fermion vertex diverges at the same $\bar{\omega}_m^* = \Lambda e^{-\pi/(2\sqrt{\lambda})}$ that we obtained before.

In the opposite limit $B \ll 1$, we use that $Y_1(2/B^{1/2}) \gg J_1(2/B^{1/2})$. Keeping only $Y_1(2/B^{1/2})$ in (36), we obtain

$$V_{SC}(L) = \frac{\gamma}{B^{1/2}} e^{\gamma L/2} \frac{J_1\left(\frac{2}{B^{1/2}} e^{\gamma L/2}\right)}{J_0\left(\frac{2}{B^{1/2}} e^{\gamma L/2}\right)} \quad (38)$$

The 4-fermion vertex now diverges at the first zero of $J_0(p)$, i.e., at

$$\frac{2}{B^{1/2}} \left(\frac{\bar{\Lambda}}{|\bar{\omega}_m|} \right)^{\gamma/2} = \frac{2}{(\gamma\lambda z)^{1/2}} \approx 2.4 \quad (39)$$

Solving for $\bar{\omega}_m$, we obtain $\bar{\omega}_m^* = (z^*)^{1/\gamma} \sim \bar{\omega}_{max}(1/\gamma)^{1/\gamma}$. This agrees the result of our earlier analysis of the case $\bar{\Lambda} \rightarrow \infty$ and $\gamma > 0$.

VII. CONCLUSIONS

The goal of this work was to analyze the crossover from a conventional BCS pairing by a massive boson to a pairing at a quantum-critical point towards some particle-hole order, when the pairing boson becomes massless. We considered a subset of quantum-critical models, in which the pairing boson is a slow mode compared to fermions, and an effective low-energy theory is purely dynamical, with an effective dynamical interaction $V(\Omega_m) \propto 1/|\Omega_m|^\gamma$, up to some upper cutoff Λ . The case $\gamma = 0$ corresponds to BCS theory of pairing from a Fermi liquid. We considered the pairing at a small, but finite γ , when the normal state is a NFL, and the case $\gamma = 0+$, when $V(\Omega_m) \propto \log \Lambda/|\Omega_m|$, and the normal state is marginal Fermi liquid. We demonstrated that for $\gamma = 0+$, the pairing instability can still be detected by summing up series of Cooper logarithms, but for a finite γ one needs to go beyond the leading logarithmic approximation to analyze the pairing. We argued that in this last case, the pairing occurs only if the interaction exceeds some finite threshold. We approximated the original integer gap equation by the differential one and solved it. This allowed us to identify the threshold at $\gamma > 0$ and the frequency scale, associated with superconductivity, once the interaction exceeds the threshold. We found the crossover between the pairing at a finite γ and at $\gamma = 0+$ and identified the parameter responsible for the crossover. We obtained the same crossover by analyzing the non-BCS RG equation for the running 4-fermion pairing vertex.

ACKNOWLEDGMENTS

We thank B. Altshuler, A. Finkelstein, S. Karchu, S. Kivelson, I. Mazin, M. Metlitski, V. Pokrovsky, S. Raghu, S. Sachdev, T. Senthil, J. Schmalian, D. Son, G. Torroba, E. Yuzbashyan, C. Varma, Y. Wang, Y. Wu, and S-S Zhang for useful discussions. The work by AVC was supported by the NSF DMR-1834856. AVC acknowledges the hospitality of KITP at UCSB, where part of the work has been conducted. The research at KITP is supported by the National Science Foundation under Grant No. NSF PHY-1748958.

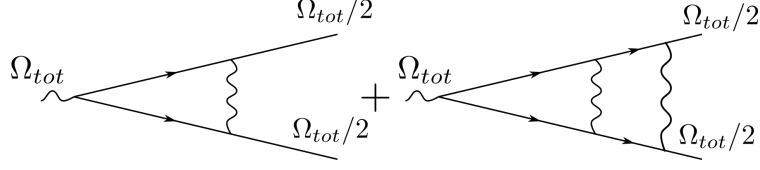


FIG. 5. Diagrammatic representation of one-loop and two-loop renormalization of the pairing vertex Φ_0 for the case $\gamma = 0+$. Solid lines are propagators of free fermions, wavy lines are $V(\bar{\Omega}_m) = \lambda \log \bar{\Lambda}/|\bar{\Omega}_m|$, and the two-fermion vertices are Φ_0 . For definiteness, we set the frequencies of external fermions to be $\Omega_{tot}/2$.

Appendix A: Derivation of Eq. (12)

In this Appendix we present some details of the derivation of order-by-order logarithmic renormalization of the pairing vertex $\bar{\Phi}(\bar{\Omega}_{tot})$ for the case $\gamma = 0+$. The Eliashberg equation for $\bar{\Phi}(\bar{\Omega}_{tot})$ is Eq. (9). Adding a constant $\bar{\Phi}_0$ to the r.h.s. and expanding in powers of the coupling λ , we obtain the series in $\lambda \log^2 \frac{\bar{\Lambda}}{|\bar{\Omega}_{tot}|}$, where, we remind, $\bar{\Lambda}$ in the upper cutoff, and all quantities are in units of our base energy \bar{g} . As we discussed in the main text, fermionic self-energy (the log term in the denominator of (9)) is small at relevant $\log \frac{\bar{\Lambda}}{|\bar{\Omega}_{tot}|} \sim 1/\sqrt{\lambda}$ and can be safely neglected.

We show the calculations at one-loop and two-loop order. The corresponding renormalizations are graphically presented in Fig. 5. In this Figure, the two-fermion vertex is $\bar{\Phi}_0$, the wavy line is $V(\bar{\Omega}_m) = \lambda \log \frac{\bar{\Lambda}}{|\bar{\Omega}_m|}$, and we set both external frequencies to be $\bar{\Omega}_{tot}/2$. The one-loop result is obtained by integrating over a single internal frequency and is

$$\lambda \int_{|\bar{\Omega}_{tot}|}^{\bar{\Lambda}} \frac{d\bar{\omega}_m}{\bar{\omega}_m} \log \frac{\bar{\Lambda}}{|\bar{\omega}_m|} = \frac{\lambda}{2} \left(\log \frac{\bar{\Lambda}}{|\bar{\Omega}_{tot}|} \right)^2 \quad (\text{A1})$$

At two-loop order we have to integrate over two internal frequencies $\bar{\omega}_m$ and $\bar{\omega}'_m$. We introduce $\bar{\omega}_m = \bar{\Omega}_{tot}x$, $\bar{\omega}'_m = \bar{\Omega}_{tot}y$ and use the fact that the leading logarithm comes from $x, y \gg 1$. Taking this limit, we obtain the two-loop correction to $\bar{\Phi}_0$ in the form

$$\lambda^2 \int_{\sim 1}^{\bar{\Lambda}/|\bar{\Omega}_{tot}|} \frac{dx}{x} \int_{\sim 1}^{\bar{\Lambda}/|\bar{\Omega}_{tot}|} \frac{dy}{y} \left[\left(\log \frac{\bar{\Lambda}}{|\bar{\Omega}_{tot}|} + \log \frac{1}{x} \right) \left(\log \frac{\bar{\Lambda}}{|\bar{\Omega}_{tot}|} + \frac{1}{2} \log \frac{1}{|x-y|} + \frac{1}{2} \log \frac{1}{x+y} \right) \right] \quad (\text{A2})$$

A simple analysis shows that the highest power of $\log \frac{\bar{\Lambda}}{|\bar{\Omega}_{tot}|}$ comes from the ranges $x \gg y$

and $y \gg x$. Evaluating the contributions from these regions, we obtain

$$\begin{aligned}
& \int_{\sim 1}^{\bar{\Lambda}/|\bar{\Omega}_{tot}|} \frac{dx}{x} \int_{\sim 1}^{\bar{\Lambda}/|\bar{\Omega}_{tot}|} \frac{dy}{y} \left[\log \frac{1}{x} \left(\frac{1}{2} \log \frac{1}{|x-y|} + \frac{1}{2} \log \frac{1}{x+y} \right) \right] = \frac{3}{8} \left(\log \frac{\bar{\Lambda}}{|\bar{\Omega}_{tot}|} \right)^4 \\
& \frac{1}{2} \log \frac{\bar{\Lambda}}{|\bar{\Omega}_{tot}|} \times \int_{\sim 1}^{\bar{\Lambda}/|\bar{\Omega}_{tot}|} \frac{dx}{x} \int_{\sim 1}^{\bar{\Lambda}/|\bar{\Omega}_{tot}|} \frac{dy}{y} \left(\log \frac{1}{|x-y|} + \log \frac{1}{x+y} \right) = -\frac{2}{3} \left(\log \frac{\bar{\Lambda}}{|\bar{\Omega}_{tot}|} \right)^4 \\
& \log \frac{\bar{\Lambda}}{|\bar{\Omega}_{tot}|} \times \int_{\sim 1}^{\bar{\Lambda}/|\bar{\Omega}_{tot}|} \frac{dx}{x} \int_{\sim 1}^{\bar{\Lambda}/|\bar{\Omega}_{tot}|} \frac{dy}{y} \log \frac{1}{x} = -\frac{1}{2} \left(\log \frac{\bar{\Lambda}}{|\bar{\Omega}_{tot}|} \right)^4
\end{aligned} \tag{A3}$$

Collecting all contributions, we obtain for the two-loop renormalization

$$A\lambda^2 \left(\log \frac{\bar{\Lambda}}{|\bar{\Omega}_{tot}|} \right)^4, \quad A = 1 - \frac{1}{2} - \frac{2}{3} + \frac{3}{8} = \frac{5}{24} \tag{A4}$$

This leads to Eq. (12) in the main text.

-
- ¹ A. T. Zheleznyak, V. M. Yakovenko, and I. E. Dzyaloshinskii, Phys. Rev. B **55**, 3200 (1997).
² I. E. Dzyaloshinskii, Sov. Phys. JETP **66**, 848 (1987).
³ I. E. Dzyaloshinskii and V. M. Yakovenko, International Journal of Modern Physics B **02**, 667 (1988), <https://doi.org/10.1142/S0217979288000494>.
⁴ P. Monthoux, D. Pines, and G. G. Lonzarich, Nature **450**, 1177 (2007).
⁵ D. J. Scalapino, Rev. Mod. Phys. **84**, 1383 (2012).
⁶ M. R. Norman, “Novel superfluids,” (Oxford University Press, 2014) Chap. Unconventional superconductivity.
⁷ S. Maiti and A. V. Chubukov, “Novel superfluids,” (Oxford University Press, 2014) Chap. Superconductivity from repulsive interaction.
⁸ B. Keimer, S. A. Kivelson, M. R. Norman, S. Uchida, and J. Zaanen, Nature **518**, 179 (2015).
⁹ T. Shibauchi, A. Carrington, and Y. Matsuda, Annual Review of Condensed Matter Physics **5**, 113 (2014).
¹⁰ R. M. Fernandes and A. V. Chubukov, Reports on Progress in Physics **80**, 014503 (2016).
¹¹ E. Fradkin, S. A. Kivelson, M. J. Lawler, J. P. Eisenstein, and A. P. Mackenzie, Annual Review of Condensed Matter Physics **1**, 153 (2010).
¹² K.-Y. Yang, T. M. Rice, and F.-C. Zhang, Phys. Rev. B **73**, 174501 (2006).
¹³ L. Fratino, P. Sémon, G. Sordi, and A.-M. S. Tremblay, Scientific Reports **6**, 22715 (2016).
¹⁴ S. Sachdev, Reports on Progress in Physics **82**, 014001 (2018).

- ¹⁵ P. Coleman, *Introduction to Many-Body Physics* (Cambridge University Press, 2015).
- ¹⁶ Y. Cao, V. Fatemi, S. Fang, K. Watanabe, T. Taniguchi, E. Kaxiras, and P. Jarillo-Herrero, *Nature* **556**, 43 (2018).
- ¹⁷ A. Abanov and A. V. Chubukov, *Phys. Rev. B* **102**, 024524 (2020).
- ¹⁸ G. M. Eliashberg, *JETP* **11**, 696 (1960), [*ZhETF*, **38**, 966, (1960)].
- ¹⁹ Y.-M. Wu, A. Abanov, and A. V. Chubukov, “Interplay between superconductivity and non-fermi liquid at a quantum-critical point in a metal. iv: The γ model and its phase diagram at $1 < \gamma < 2$,” (2020), arXiv:2009.10911 [cond-mat.supr-con].
- ²⁰ D. F. Mross, J. McGreevy, H. Liu, and T. Senthil, *Phys. Rev. B* **82**, 045121 (2010).
- ²¹ M. A. Metlitski, D. F. Mross, S. Sachdev, and T. Senthil, *Phys. Rev. B* **91**, 115111 (2015).
- ²² S. Raghu, G. Torroba, and H. Wang, *Phys. Rev. B* **92**, 205104 (2015).
- ²³ R. Mahajan, D. M. Ramirez, S. Kachru, and S. Raghu, *Phys. Rev. B* **88**, 115116 (2013); A. L. Fitzpatrick, S. Kachru, J. Kaplan, and S. Raghu, *Phys. Rev. B* **88**, 125116 (2013); *Phys. Rev. B* **89**, 165114 (2014); G. Torroba and H. Wang, *Phys. Rev. B* **90**, 165144 (2014); A. L. Fitzpatrick, G. Torroba, and H. Wang, *Phys. Rev. B* **91**, 195135 (2015), and references therein.
- ²⁴ H. Wang, S. Raghu, and G. Torroba, *Phys. Rev. B* **95**, 165137 (2017).
- ²⁵ H. Wang, Y. Wang, and G. Torroba, *Phys. Rev. B* **97**, 054502 (2018).
- ²⁶ A. L. Fitzpatrick, S. Kachru, J. Kaplan, S. Raghu, G. Torroba, and H. Wang, *Phys. Rev. B* **92**, 045118 (2015).
- ²⁷ Y. Wang and A. V. Chubukov, *Phys. Rev. Lett.* **110**, 127001 (2013).
- ²⁸ Y.-M. Wu, A. Abanov, and A. V. Chubukov, *Phys. Rev. B* **99**, 014502 (2019).
- ²⁹ D. T. Son, *Phys. Rev. D* **59**, 094019 (1999).
- ³⁰ A. V. Chubukov and J. Schmalian, *Phys. Rev. B* **72**, 174520 (2005).
- ³¹ T. Schäfer and F. Wilczek, *Phys. Rev. D* **60**, 114033 (1999).
- ³² R. D. Pisarski and D. H. Rischke, *Phys. Rev. D* **61**, 051501 (2000).
- ³³ Q. Wang and D. H. Rischke, *Phys. Rev. D* **65**, 054005 (2002).
- ³⁴ J. A. Damia, M. Solís, and G. Torroba, *Phys. Rev. B* **102**, 045147 (2020).
- ³⁵ D. V. Khveshchenko, *Journal of Physics: Condensed Matter* **21**, 075303 (2009).
- ³⁶ C. M. Varma, P. B. Littlewood, S. Schmitt-Rink, E. Abrahams, and A. E. Ruckenstein, *Phys. Rev. Lett.* **63**, 1996 (1989); P. B. Littlewood and C. M. Varma, *Phys. Rev. B* **46**, 405 (1992).
- ³⁷ C. M. Varma, *Rev. Mod. Phys.* **92**, 031001 (2020).

- ³⁸ A. Abanov, A. V. Chubukov, and J. Schmalian, *Advances in Physics* **52**, 119 (2003).
- ³⁹ A. Abanov, A. V. Chubukov, and J. Schmalian, *Journal of Electron spectroscopy and related phenomena* **117**, 129 (2001).
- ⁴⁰ A. A. Abrikosov, L. P. Gorkov, and I. E. Dzyaloshinski, *Methods of Quantum Field Theory in Statistical Physics* (Pergamon Oxford, 1965).
- ⁴¹ A. Abanov, A. V. Chubukov, and A. M. Finkel'stein, *EPL (Europhysics Letters)* **54**, 488 (2001).
- ⁴² Y. Wang, A. Abanov, B. L. Altshuler, E. A. Yuzbashyan, and A. V. Chubukov, *Phys. Rev. Lett.* **117**, 157001 (2016).
- ⁴³ A. Abanov, Y.-M. Wu, Y. Wang, and A. V. Chubukov, *Phys. Rev. B* **99**, 180506 (2019); Y.-M. Wu, A. Abanov, Y. Wang, and A. V. Chubukov, *Phys. Rev. B* **99**, 144512 (2019).
- ⁴⁴ The extension to $N > 1$ was originally rationalized by extending the original model to matrix $SU(N)$, with integer N , hence the notation. We treat N as a continuous parameter.
- ⁴⁵ E. A. Yuzbashyan, A. V. Chubukov, A. Abanov, and B. L. Altshuler, “Non BCS pairing near a quantum phase transition – effective mapping to a spin chain,” In preparation.
- ⁴⁶ Y.-M. Wu, A. Abanov, Y. Wang, and A. V. Chubukov, *Phys. Rev. B* **102**, 024525 (2020).